J. Phys.: Condens. Matter 7 (1995) 3881–3894. Printed in the UK

Charge-transfer spectra and dynamics of $CuBr_4^{2-}$ in $[N(CH_3)_4]_2CdBr_4$:Cu^{2+} crystals: a new first-order phase transition at $T_{c2} = 20$ K

R Valiente, M C Marco de Lucas and F Rodríguez

DCITTYM (Sección Ciencia de Materiales), Facultad de Ciencias, Universidad de Cantabria, 39005 - Santander, Spain

Received 1 December 1995

Abstract. The charge-transfer electronic structure of $CuBr_4^{2-}$ in $[N(CH_3)_4]_2CdBr_4$ crystals is investigated through polarized optical absorption spectroscopy. The transition energy and the band polarization are explained in terms of the Jahn–Teller distortions of D_{2d} symmetry of the $CuBr_4^{2-}$ complex. Some bands are split in the low-temperature spectra by the spin–orbit interaction of the Br ligands. The results are compared with those available for other $CuBr_4^{2-}$ systems. We also investigate the dynamics of the inorganic $CuBr_4^{2-}$ units in the 9.5–300 K temperature range through the intensity of the charge-transfer bands. Analogously to the $CdBr_4^{2-}$ tetrahedra in the pure crystal, $CuBr_4^{2-}$ experiences reorientational motions upon varying the temperature which are correlated with the temperature dependence of the monoclinic β parameter below the $Pmcn \rightarrow P2_1/c$ phase transition temperature $T_{c1} = 272$ K. An important finding of the present work is the observation of anomalies in the $CuBr_4^{2-}$ dynamics which are associated with the existence of a new first-order phase transition at $T_{c2} = 20$ K with a thermal hysteresis $\Delta T = 10$ K. This new phase transition, which had not previously been detected in the $[(CH_3)_4N]_2MBr_4$ (M = Zn, Mn, Co or Cd) series, would correspond to the monoclinic $P2_1/c$ to orthorhombic $P2_12_12_1$ transition, confirming the predictions of the universal p–T phase diagrams of the title compounds.

1. Introduction

Copper bromide crystals are attractive systems as potential candidates for thermochroic and piezochroic materials. In the case of tetrabromide $CuBr_4^{2-}$ complexes, the optical absorption (OA) spectrum is dominated by the highly polarized $Br^- \rightarrow Cu^{2+}$ charge transfer (CT) bands, whose intensity and transition energy strongly depend on the orientation as well as on the degree of the Jahn–Teller (JT) distortion displayed by such $CuBr_4^{2-}$ complexes [1–4]. Thus structural modifications induced either by temperature or by pressure can lead to significant changes in the optical properties of such systems. Furthermore, it must be remarked that CT transitions of Cu^{2+} complexes are in general much more sensitive than the intraconfigurational d^9 transitions to changes in the Cu–ligand distance or the JT distortion angle, as has been shown for $CuCl_4^{2-}$ [5, 6]. A similar behaviour is expected for the much less studied $CuBr_4^{2-}$ [1, 2, 4]. In fact, the CT spectrum of $CuBr_4^{2-}$ deserves for more detailed investigation in order to clarify the nature of the intense polarized CT bands of these JT distorted complexes.

The aim of this paper is to investigate the CT spectrum of Cu^{2+}-doped TMA_2CdBr_4 (TMA = $N(CH_3)_4$) crystals and their temperature dependence in order to establish correlations with the local symmetry and the orientation of the tetrahedral distorted $CuBr_4^{2-}$

0953-8984/95/203881+14$19.50

complex. This work follows a previous study upon the optical properties of $CuBr_4^{2-}$ formed in TMA_2MnBr_4:Cu^{2+} [4]. In this system, the overlapping between the $CuBr_4^{2-}$ CT bands and the crystal-field bands of $MnBr_4^{2-}$ prevented a complete study of the CT spectra, particularly at low temperatures. This limitation has been overcome using the isomorphous cadmium crystal which is transparent in the $Br^- \rightarrow Cu^{2+}$ CT region and allows easy replacement of Cd by Cu. A similar procedure was recently employed to obtain the polarized CT spectra of hexacoordinated CuX_6^{4-} complexes in $TMACdX_3$ (X = Cl or Br) [7].

An interesting feature is the structural phase transition (PT) sequence displayed by the TMA_2MX_4 crystal family. In particular, the TMA_2CdBr_4 crystal ($\beta-K_2SO_4$-type structure) undergoes an orthorhombic to monoclinic ($Pmcn \rightarrow P12_1/c1$) structural PT at $T_{c1} = 272$ K [8–10] which is mainly associated with rotations and displacements of both the organic and the inorganic tetrahedra [11]. This aspect is of interest for the present study since CT bands may exhibit significant intensity changes as a consequence of the $CuBr_4^{2-}$ reorientations induced either by temperature in the monoclinic phase or around the phase transition temperature. The influence of this PT upon the optical properties will be analysed in this work in order to explore the dynamics of the inorganic $CuBr_4^{2-}$ tetrahedra. Evidence for the existence of a new first-order PT at $T_{c2} = 20$ K with a thermal hysteresis $\Delta T = 10$ K, is given in this work. Although unusual, the existence of such a PT at a low temperature confirms the expectations on the basis of the universal p-T phase diagram available for the family of TMA_2MX_4 crystals which foresees another monoclinic $P2_1/c \rightarrow$ orthorhombic $P2_12_12_1$ PT for bromides at lower temperatures [12–15]. To our knowledge, this finding would be the first case where a second PT has been detected among the TMA_2MBr_4 (M = Mn, Cd, Zn or Co) family, indicating the usefulness of the CT spectra of Cu^{2+} as probes for detecting structural PTs. Previous work on Cu^{2+}-doped TMA_2MnCl_4 [6, 16], $TMACdX_3$ [7] and the mixed $NH_4Cl_xBr_{1-x}$ ($x = 0$–1) crystals [17–22] confirm this view.

Apart from the influence of the PTs, the thermochroism exhibited by this crystal is noteworthy. Its colour progressively changes from violet at room temperature to slightly reddish at low temperatures as a consequence of the sharpening of the first CT triplet.

2. Experimental details

Single crystals of TMA_2CdBr_4:Cu^{2+} were grown by slow evaporation as described elsewhere [23]. 0.5 mol% of copper halide was added to the solutions. The real Cu^{2+} concentration, $[Cu^{2+}] \simeq 700$ ppm was measured by atomic absorption spectroscopy.

The orthorhombic (*Pmcn*) crystallographic structure at room temperature was checked by x-ray diffraction. Several *c* and *a* plates were selected and polished for optical studies. The crystals were oriented by means of a polarizing microscope according to the structural data of [23].

Spectra were recorded with a Lambda 9 Perkin–Elmer spectrophotometer equipped with Glan Taylor polarizing prisms. Sample path lengths for absorption varied from about 0.5 to 1 mm. The temperature was stabilized to within 0.05 K in the 9.5–300 K range with a Scientific Instruments 202 closed-circuit cryostat and an APD-K controller.

3. Results

Figures 1 and 2 depict the polarized OA spectra of the Cu doped TMA_2CdBr_4 along the *a*, *b* and *c* orthorhombic directions at 300 and 9.5 K. The room-temperature spectra consist

of four groups of highly polarized bands denoted A, B, C and C′ which are located at 17900 cm^{-1}, 28200 cm^{-1}, 36000 cm^{-1} and 23450 cm^{-1}, respectively. Note that the maximum and minimum intensities for C and the shoulder C′ are found when E is parallel to a and b, respectively, while the opposite occurs for bands A and B. Their relative intensity, defined as

$$I_{ri}^{j} = I_i^j \Big/ \sum_{i=a,b,c} I_i^j \tag{1}$$

where I_i^j is the integrated intensity of band j = A, B and C in the polarized $i = a$, b and c spectrum, is given in table 1. At $T = 9.5$ K, the spectra show a rich band structure which is hidden at room temperature. While C remains a single band, bands A and B exhibit a triplet structure, each component A_k or B_k ($k = 1,2,3$) having nearly the same polarization behaviour. The weak band C′, at 23450 cm^{-1}, is well-resolved at low temperatures. The transition energy of each component, the polarization and the total oscillator strength are collected in table 2. The oscillator strength is obtained through

$$f = 3.89 \times 10^{-8} \frac{n}{(n^2+2)^2} \int \varepsilon \, dE \tag{2}$$

where ε is the molar extinction coefficient, E (cm^{-1}) is the transition energy and $n = 1.57$ is the refractive index [23]. It should be noted that the relative band intensities in the low-temperature spectra change from sample to sample depending on the crystal face and its thermal history. By contrast, the spectrum along a given a, b or c polarization above the PT temperature $T_{c1} = 272$ K is always the same irrespective of the sample employed. The different relative intensity variations found in the OA spectra at $T = 9.5$ K, as we shall see later, seem to be associated with the monoclinic domain structure exhibited by the crystal below T_{c1}.

Table 1. Square components e_1, e_2 and e_3 of the unitary vectors e_1, e_2 and e_3 pointing along the S_4 axes of the MBr_4^{2-} tetrahedra in the pure TMA_2MBr_4 (M = Cu or Cd) crystals with respect to the orthorhombic a, b and c directions, respectively [11, 32]. I_{ri}^j, with $i = a$, b and c, are the relative intensities of bands j = A, B and C, defined in equation (1). The last two columns show the polarization type of the bands: x, y polarization, for bands A and B, and z polarization for band C: $I_{ri}^{C} = \cos^2\theta_i$ and $I_{ri}^{A \text{ or } B} = (\sin^2\theta_i)/2$, where θ_i is the angle that the distortion axis makes with $i = a$, b or c.

	$CuBr_4^{2-}$			$CdBr_4^{2-}$							
i direction	e_1	e_2	e_3	e_1	e_2	e_3	I_{ri}^{C}	I_{ri}^{B}	I_{ri}^{A}	$I_{ri}^{C} + 2I_{ri}^{A}$	$I_{ri}^{C} + 2I_{ri}^{B}$
a	0.02	0.52	0.46	0.01	0.61	0.38	0.49	0.25	0.23	0.99	0.95
b	0.62	0.14	0.24	0.63	0.12	0.25	0.16	0.44	0.45	1.04	1.06
c	0.36	0.34	0.30	0.36	0.27	0.37	0.35	0.31	0.32	0.97	0.99

The temperature dependences of different spectroscopic parameters in the 9.5–300 K range are shown in figures 3–5. It is interesting to observe that, while band C experiences a typical blue shift of about 400 cm^{-1} from 300 to 9.5 K, its intensity displays enormous variations in the same temperature range (figure 4). In particular, this intensity in b polarization at $T = 225$ K becomes almost twice the room-temperature intensity at the expense of the corresponding decrease undergone by the intensity in polarization a.

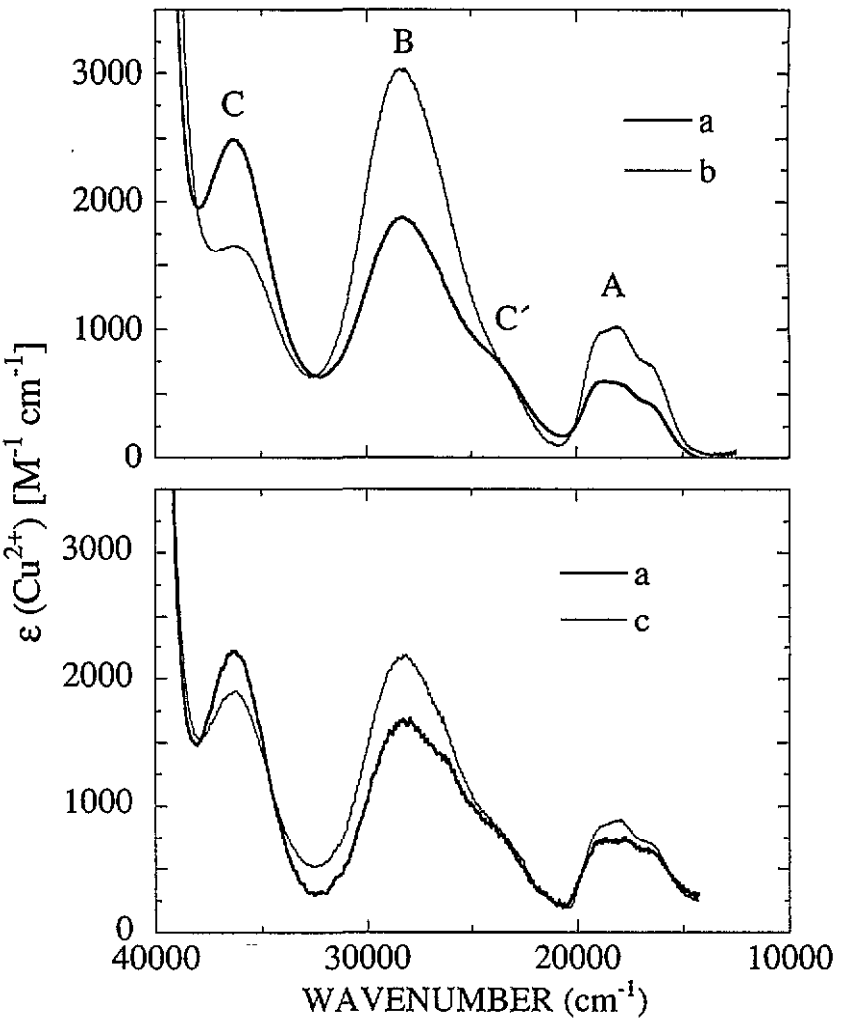

Figure 1. Polarized OA spectra of $TMA_2CdBr_4:Cu^{2+}$ at $T = 300$ K. Suitable *c* and *b* single-crystal plates were used for obtaining the spectra along the *a* and *b*, and *a* and *c* orthorhombic directions, respectively.

Opposite behaviours are also found for bands A and B. Nevertheless, the $I(T)$ curves depicted in figure 4 correspond to the highest variations observed among different *c* and *b* plates investigated. Although in all cases the intensities in *a* and *b* polarization exhibit similar behaviours with temperature, their variations are usually much smaller than those shown in figure 4. The weakest variation for the C intensity along *a* is found in the *b* plates where a dense structure of the two types of monoclinic domain is present at low temperatures.

The occurrence of the $Pmcn \rightarrow P12_1/c1$ structural PT is evidenced by the progressive change in the $\partial I/\partial T$ slope, below $T_{c1} = 272$ K. The weak temperature dependence of the intensity just around T_{c1} is probably due to the second-order character of the PT [9, 10]. The abrupt jump experienced by the intensity at $T = 20$ K upon heating is noteworthy. Such a jump, observed at 10 K in the cooling run, has been associated with the existence of a new PT

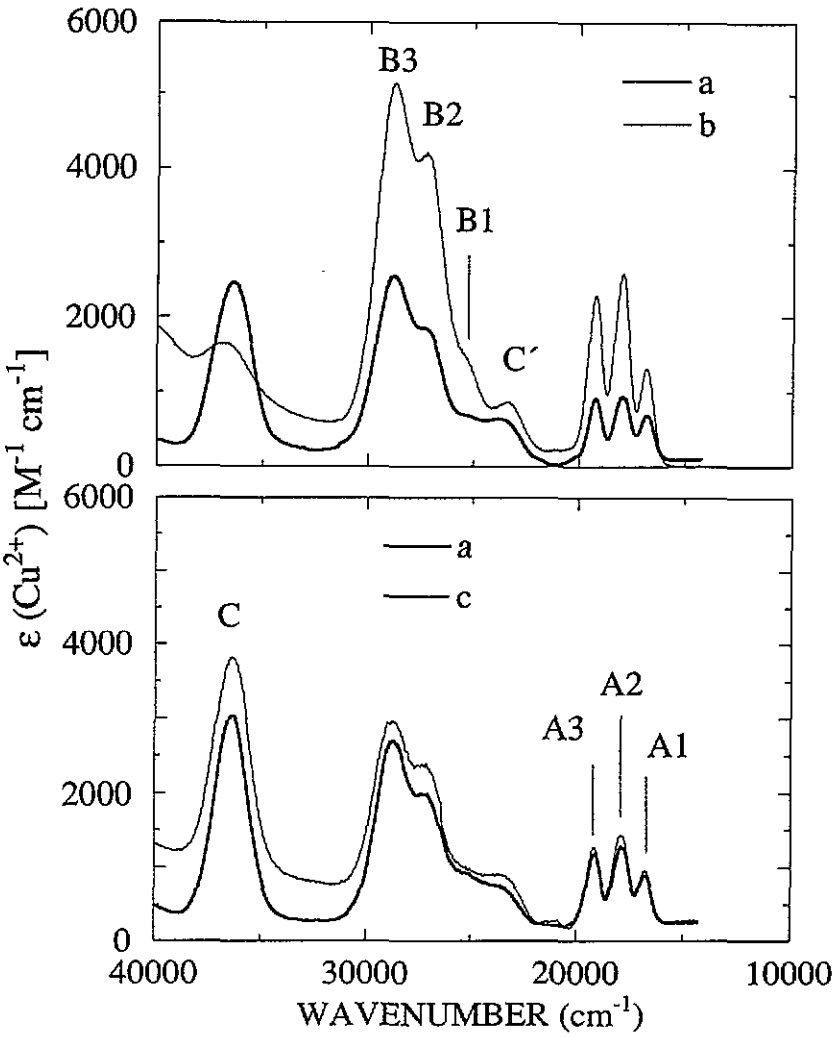

Figure 2. Polarized OA spectra of $TMA_2CdBr_4:Cu^{2+}$ at $T = 9.5$ K. The polarization is that given in figure 1.

in the host crystal. Figure 5 shows a magnification of this variation along the a polarization (c plate) in the 9.5–30 K range. Although the sign and the magnitude of this jump are sample dependent, as is pointed out by comparing the $I(T)$ curves (c plate) and OA spectra (b plate) given in the inset, the measured transition temperature and the corresponding thermal hysteresis $\Delta T = 10$ K, are identical in every case. Note that the increase in the band-C intensity above 20 K shown in the inset contrasts with the observations on the $I(T)$ curves for the c plate. This increase, which is accompanied by an analogous decrease in the A and B intensities for the spectrum polarized along a, is not observed in the c spectrum which remains almost unaffected by this new PT. It must also be pointed out that this anomaly at T_{c2} is not only a local effect. In fact, although the PT was explored using Cu impurities as optical probes, we have analogously observed small jumps in the background absorption of the host crystal at the same temperature. Finally, the maxima and

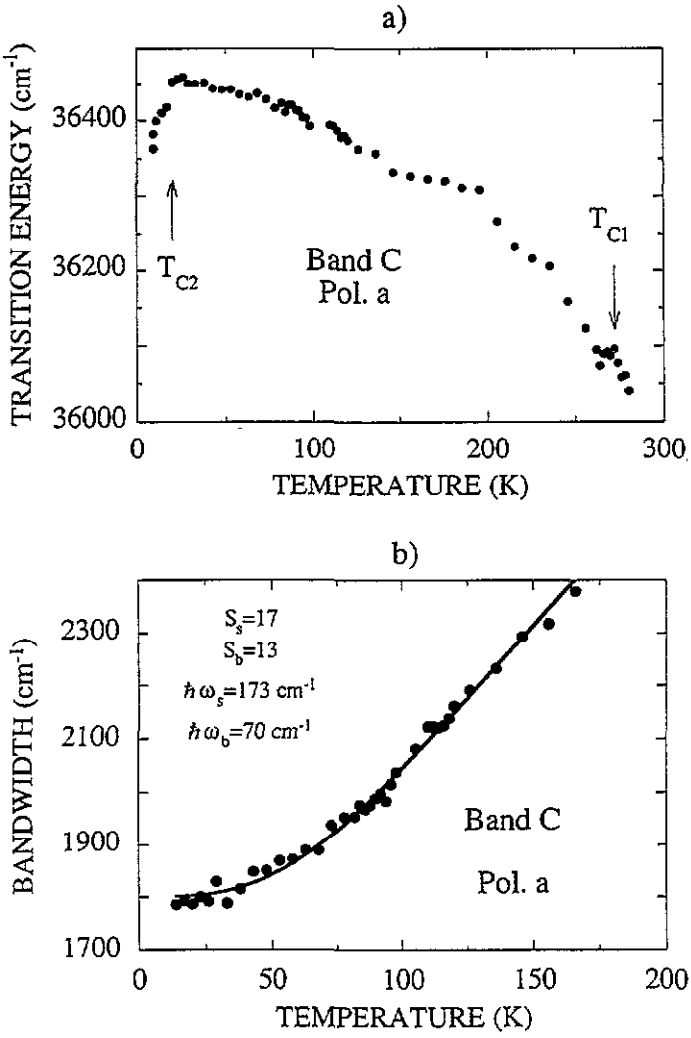

Figure 3. Variation in (*a*) the transition energy and (*b*) the band width of band C obtained from the OA spectrum polarized along *a* by moment analysis in the 9.5–300 K temperature range.

minima observed in the $I(T)$ curves of figure 4 in both the heating and the cooling runs, as discussed later, seem to be associated with no PT, given that the corresponding OA spectra taken around these temperatures show neither abrupt jumps nor hysteresis in the variation of the band intensity and transition energy.

4. Analysis and discussion

4.1. Electronic structure of $CuBr_4^{2-}$

The OA spectra of $TMA_2CdBr_4:Cu^{2+}$ shown in figures 1 and 2 are very similar to those previously found for the isomorphous $TMA_2MnBr_4:Cu^{2+}$ [4], but two significant differences must be pointed out. Firstly, at variance with the Mn crystal, the OA spectra in the present

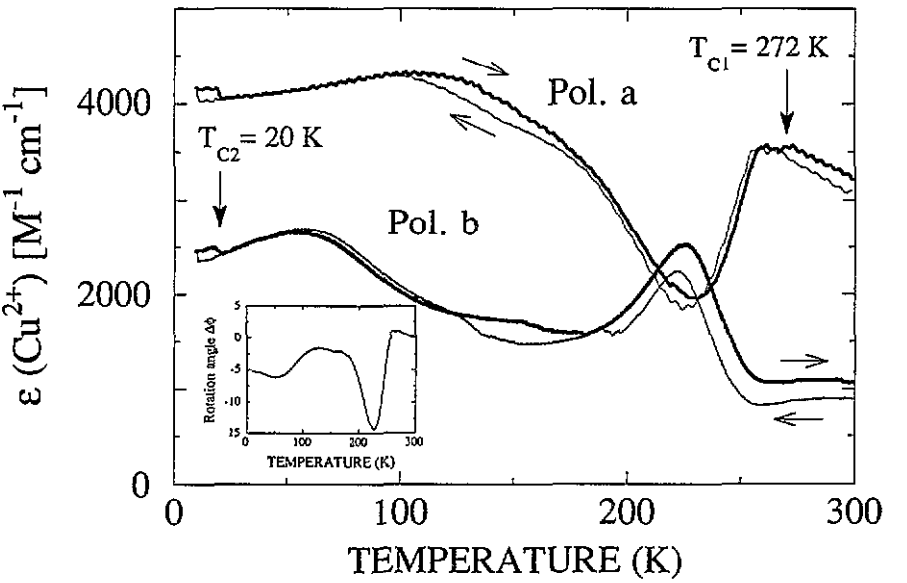

Figure 4. Continuous plot of the band-C absorption intensity versus temperature for the *a* and *b* polarizations (*c* plate), for two different heating–cooling cycles. A constant-absorption background has been subtracted in order to obtain the relative intensity given in table 1. The heating and cooling rates were 3 K min^{-1}. The inset shows the variation in the rotation angle $\Delta\phi$ of $CuBr_4^{2-}$ with temperature (see text for explanation). The vertical arrows indicate the PT temperatures.

case are only due to the $CuBr_4^{2-}$ complex. Secondly, while band C shows the maximum and minimum intensities along the *b* and *a* directions, respectively, in the Mn crystal, the opposite occurs for the present system. An inverse behaviour is also observed for bands A and B. The first difference is relevant because it allows us to reveal the splitting of band B by the spin–orbit interaction of the Br ligands in the low-temperature spectra. Such splitting could not be observed in band B in TMA_2MnBr_4:Cu^{2+} owing to the sharp peak structure of the overlapping Mn^{2+} peaks [4]. The second point could probably reflect a distinct $CuBr_4^{2-}$ orientation within the TMA_2CdBr_4 crystal. The higher volume of the $CdBr_4^{2-}$ tetrahedron with respect to the Mn and Cu tetrahedra in their corresponding crystals could favour this different orientation.

The bands observed in figures 1 and 2 correspond to $Br^- \rightarrow Cu^{2+}$CT transitions whose energy and polarization can be explained within a D_{2d} molecular orbital (MO) framework. This symmetry, which is associated with the flattening of the coordination tetrahedra along one of the tetrahedral S_4 axes (figure 6), is usually found for CuX_4^{2-} (X = Cl or Br) in either pure [24–32] or Cu-doped [4, 6] compounds, thus indicating the relevance of the vibrational e (bending) mode in the electron–phonon coupling, leading to the JT distortion of the Cu tetrahedron.

The electric dipole CT transitions allowed in D_{2d} involve electronic jumps from σ and π bonding (mainly Br^-MO levels of e and a_1 symmetry) to the unfilled antibonding (mainly Cu^{2+} $b_2(x^2 - y^2)$MO) as indicated in the state energy diagram in figure 6. These transitions are z polarized or (x, y) polarized depending on whether the ligand MO transforms as a_1 or e, respectively. Apart from the transition energies, the assignment given in table 2 is based on the polarization of these bands. The analysis of the relative band intensity along

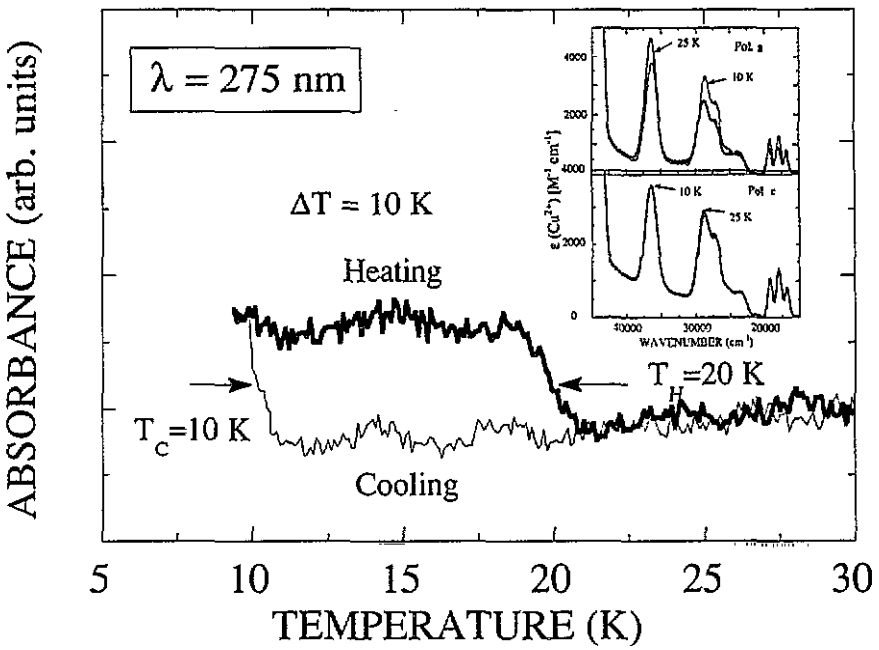

Figure 5. Magnification of the band-C intensity versus temperature plot in the 9.5–30 K range along the a direction in the heating and cooling runs. The inset shows the variation in the polarized OA spectra along the a and c directions (b plate) at 10 and 25 K. The variation in the band intensities reflects an abrupt rotation of the $CuBr_4^{2-}$ complex around the c direction at $T_{c2} = 20$ K. Note the different sign of the C intensity change along a in the b and c plates.

each polarization (table 1) clearly indicates that the corresponding CT transitions are either (x, y) polarized (bands A and B) or z polarized (bands C and C'), in agreement with the proposed D_{2d} symmetry. Here z is taken along the S_4 distortion axis, and (x, y) are two orthogonal directions (figure 6). Furthermore, we can extract valuable information about the $CuBr_4^{2-}$ orientation as well as on the S_4 axis, together with the JT distortion which takes place from I_{ri}, following the procedure employed in [4, 6]. In particular, the I_{ri}-values ($i = a$, b and c) for the z-polarized band C give directly the square components of the unitary vector along the S_4 distortion axis. These values are similar to those of the S_4 axis of the $CdBr_4^{2-}$ tetrahedra pointing along $e_2 = 0.78i + 0.35j + 0.52k$ and $e_3 = 0.62i - 0.50j - 0.61k$, thus indicating that the distortion axis in $CuBr_4^{2-}$ does not correspond to the e_1 direction of the $CdBr_4^{2-}$ tetrahedron [11]. As previously discussed, this result contrasts with that found for TMA_2MnBr_4:Cu^{2+} [4] and TMA_2MnCl_4:Cu^{2+} [6] whose distortion axes, as in the Cu isomorphous crystals, correspond to e_1. The reason for this different behaviour is probably associated with the higher volume of the $CdBr_4^{2-}$ tetrahedron whose Cd–Br distance (2.57 Å) [11] is longer than the Mn–Br and Cu–Br distances (2.45 Å [33] and 2.37 Å [32], respectively), and therefore the equilibrium conditions for $CuBr_4^{2-}$ can be substantially modified in the present TMA_2CdBr_4 crystal. The measured I_{ri}-values in table 1 can be correlated with the structural data if we consider that the $CuBr_4^{2-}$ complexes distort along the e_3 S_4 axis and rotate 10° around the orthorhombic c axis. Although other alternatives can be used to explain the observed room-temperature intensities such as equal distortions along e_3 and e_2 or only along e_2 followed by small rotations around an axis on the a plane, the proposed interpretation is the most likely according to the C intensity

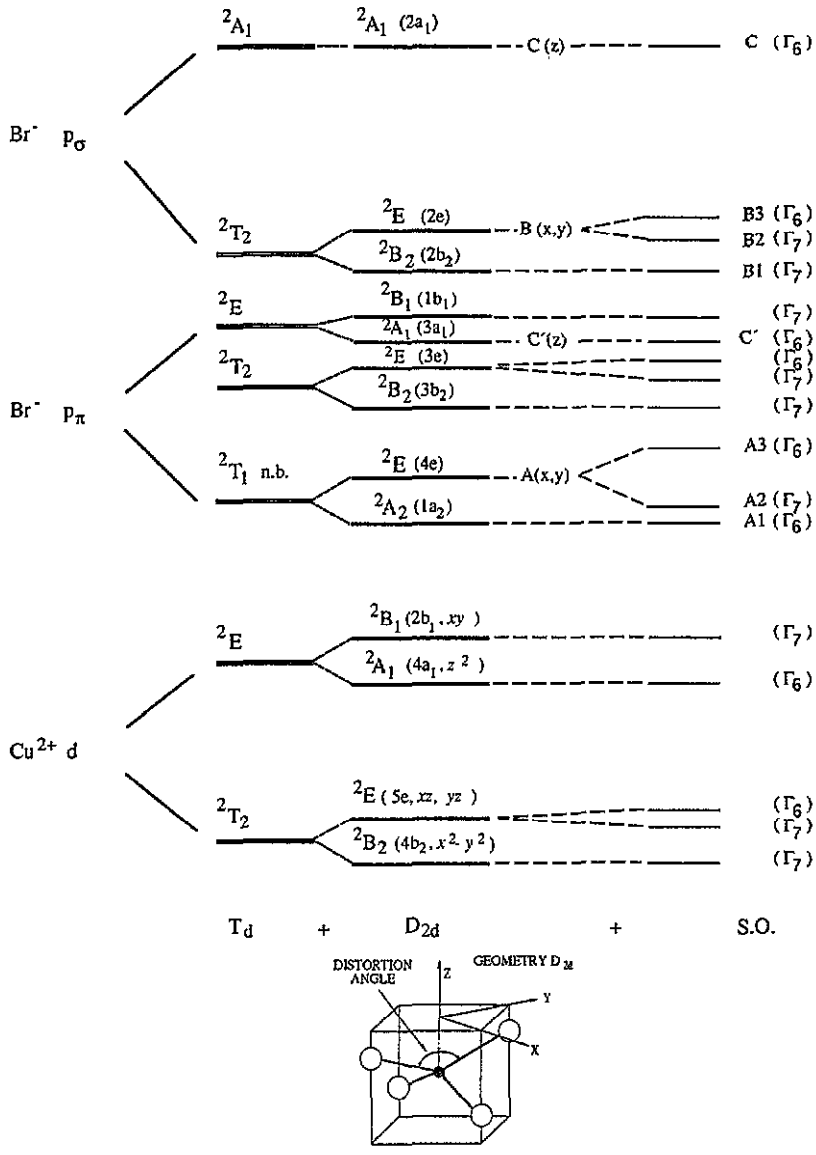

Figure 6. Energy level diagram of the $CuBr_4^{2-}$ electronic states in T_d symmetry and under the influence of a D_{2d} distortion and the spin–orbit interaction of the Br^- ligands [4]. The assignment of the observed CT bands as well as their polarizations are included. The x, y, z coordinates are indicated in the figure.

thermal dependence depicted in figure 4.

The comparison between the CT transition energies of the present system and Mn which is isomorphous at 300 K strongly suggests that the local structure around the Cu^{2+} impurity is essentially the same in both systems in spite of the large difference between the volumes of the Mn and Cd tetrahedra. It can therefore be concluded that the chemical pressure effect in $CuBr_4^{2-}$ does not seem to influence the Cu–Br distance very much as could be expected

Table 2. The CT band assignment of $CuBr_4^{2-}$ in $TMA_2CdBr_4:Cu^{2+}$. The corresponding data for $TMA_2MnBr_4:Cu^{2+}$ [4] are also included. f is the experimental oscillator strength at 300 and 9.5 K obtained in the following way: $f = f_a + f_b + f_c$ for bands C and C', and $f = (f_a + f_b + f_c)/2$ for bands A and B. $f_i (i = a, b$ and $c)$ is calculated from the i-polarized spectrum through equation (2).

				$TMA_2MnBr_4:Cu^{2+}$			$TMA_2CdBr_4:Cu^{2+}$			
				Peak energy (cm^{-1})		f	Peak energy (cm^{-1})		f	
	Transition	Type	Polarization	300 K	9.5 K	300 K	300 K	9.5 K	300 K	9.5 K
	$1a_2\ (nb) \rightarrow 4b_2$	CT			16580 (A1)	0.0032		16780 (A1)		0.003
(A)	$4e \rightarrow 4b_2$	CT	x, y	18000	17845 (A2)	0.0084	17900	17920 (A2)	0.011	0.006
					19055 (A3)	0.0061		19200 (A3)		0.005
(C')	$3a_1 \rightarrow 4b_2$	CT	z	23800		$\simeq$0.01	23450	23500	$\leqslant$0.005	0.004
	$3e \rightarrow 4b_2$	CT	x, y							
	$2b_2 \rightarrow 4b_2$	CT		—		—		25250 (B1)		$\simeq$0.003
(B)	$2e \rightarrow 4b_2$	CT	x, y	28400		0.06	28200	27000 (B2)	0.045	$\simeq$0.017
								28900 (B3)		$\simeq$0.028
(C)	$2a_1 \rightarrow 4b_2$	CT	z	36100		$\simeq$0.05	36000	36400	0.025	$\simeq$0.03

for a covalent complex with terminal ligands whose equilibrium bond distances are mainly determined by the $CuBr_4^{2-}$ molecular unit.

A salient feature of the present work is the presence of additional bands (B1, B2 and B3) at 25 250 cm^{-1}, 27 000 cm^{-1} and 28 900 cm^{-1}, respectively, in the low-temperature spectra, showing a predominant (x, y) polarization. While bands B2 and B3 correspond to the mainly σ-bonded ^2E ($\Gamma_6+\Gamma_7$) state, B1 must be associated either with the $^2B_2$ (Γ_7) state from the splitting of the parent tetrahedral $^2T_2$ state by the spin–orbit interaction or with the mainly π-bonded ^2E state. The proposed CT band assignment is given in figure 6. Note that the presence of transitions from the $^2B_2$ ground state to the $^2A_2$ and $^2B_2$ CT excited states (bands A1 and B1, respectively), which are forbidden in D_{2d}, is a consequence of the strong mixing with states of E symmetry by spin–orbit interaction of the Br ligands. This effect is clearly illustrated in the first CT triplet whose B1 component, corresponding to the $^2B_2 \rightarrow {}^2A_2$ transition, should be absent on the basis of only D_{2d} symmetry as has been observed for the corresponding $CuCl_4^{2-}$ complex [6]. Although the spin–orbit interaction allows CT transitions to be either (x, y) polarized ($\Gamma_7 \rightarrow \Gamma_7$) or (x, y, z) polarized ($\Gamma_7 \rightarrow \Gamma_6$), the bands in figures 1 and 2 show dominant (x, y) or z polarizations. The oscillator strength values (table 2) obtained from equation (2) indicate the more important contribution from the p_σ orbitals than the p_π orbitals of the Br ligands as expected by the larger overlap of the former orbitals with the mainly $Cu^{2+}b_2$ ($x^2 - y^2$) orbital. It must be noted, however, that the oscillator strengths for $TMA_2CdBr_4:Cu^{2+}$ are somewhat different from those measured for $TMA_2MnBr_4:Cu^{2+}$. These deviations are probably due to the presence of Mn^{2+} peaks which had to be extracted from the OA spectra of $TMA_2MnBr_4:Cu^{2+}$ in order to measure the integrated intensity of bands B and C [4] as well as uncertainties of about 20% in the Cu^{2+} concentration. Anyway, the presence of Mn^{2+} seems to be responsible for the large difference found between the oscillator strength of bands B and C in these systems.

4.2. Temperature dependences of the spectroscopic parameters: the influence of the structural phase transitions

The study of the temperature dependence of the $CuBr_4^{2-}$ spectra has mainly been focused on band C since its z-polarized singlet character allows direct correlation between the intensity and the orientation of the $CuBr_4^{2-}$ tetrahedra. As regards the variation in the transition energy, the band width and the intensity of band C with temperature, the following facts must be emphasized.

(1) The local structure around Cu^{2+} does not significantly change in the 9.5–300 K temperature range. This is suggested by the blue shift of 400 cm^{-1} experienced by band C in this temperature range which mainly reflects slight variations in the Cu–Br distance due to thermal expansion effects. If we assume variations ΔR of about -0.005 Å from 300 to 100 K, a blue shift of 500 cm^{-1} should be expected for these CT bands provided that $\partial E/\partial R \simeq -10^5$ cm^{-1} $Å^{-1}$. This $\partial E/\partial R$-value typically corresponds to those obtained from MS–X_α calculations for CT transitions in square planar CuX_4^{2-} (X = Cl or Br) complexes [5]. Furthermore, the reduction in the Cu–Br distance with increasing temperature could also account for the increase in the CT band intensity (about 20%) observed at low temperatures.

(2) The variation in the band width derived from moment analysis follows hyperbolic cotangent functions of the type $H(T) = H(0)[\coth(\hbar\omega_{\text{eff}}/2kT)]^{1/2}$. The fitted effective vibrational energy from the experimental data of figure 3(b) is $\hbar\omega_{\text{eff}} = 148$ cm^{-1}. Since the vibrational energy of the stretching tetrahedral a_1 mode measured by Raman spectroscopy for $CuBr_4^{2-}$ is $\hbar\omega_s = 173$ cm^{-1} [3], the present analysis indicates that the bending JT active

e_θ mode (a_1 in D_{2d}) must be involved in the thermal broadening of band C. In fact, only these two a_1 vibrational modes can be linearly coupled to this singlet–singlet $^2B_2 \rightarrow {}^2A_1$ transition within D_{2d}. We have estimated the participation of each mode in the thermal broadening of band C by fitting the experimental $H(T)$-values to the following equation (3) keeping $\hbar\omega_s = 173\ cm^{-1}$ and $\hbar\omega_b = 70\ cm^{-1}$ as fixed parameters:

$$H(T) = 2.36\left[S_s(\hbar\omega_s)^2 \coth\left(\frac{\hbar\omega_s}{2kT}\right) + S_b(\hbar\omega_b)^2 \coth\left(\frac{\hbar\omega_b}{2kT}\right)\right]^{1/2}. \qquad (3)$$

S_s and S_b are the Huang–Rhys factors associated with the stretching and bending a_1 modes, respectively. The vibrational energy, $\hbar\omega_b = 70\ cm^{-1}$ actually corresponds to the bending $\nu_2(e)$ mode of tetrahedral MBr_4^{2-} (M = Zn or Cd) measured by Raman spectroscopy for Cs_2CdBr_4 [34] and Cs_2ZnBr_4 [35]. The fitted parameters are $S_s = 17$ and $S_b = 13$. Note that, although the Huang–Rhys factors are similar for both modes, the electron–phonon coupling for the stretching mode $S_s\hbar\omega_s$ is dominant, in agreement with findings for CuX_6^{4-} (X = Cl and Br) [7] and square planar $CuCl_4^{2-}$ complexes [7, 36].

(3) The variation on the band-C intensity with temperature, depicted in figure 4, reflects the reorientational motions of the $CuBr_4^{2-}$ complexes. This behaviour resembles the lattice dynamic of the pure TMA_2CdBr_4 crystal. Structural studies by x-ray diffraction performed at different temperatures show that the inorganic tetrahedron rotates 9.4° from 272 to 158 K around an axis lying on the a plane. The variation undergone by the z-polarized band C along a and b can be analogously explained on the basis of $CuBr_4^{2-}$ rotations but around the orthorhombic c axis. This interpretation is supported by the opposite behaviours shown by the intensity in each polarization. In fact, the loss of intensity I_a in polarization a is gained by the b intensity I_b and vice versa in the 300–100 K range. Below 100 K, however, I_b and I_a are not correlated. The broad variation experienced by I_b at around 60 K is not observed for I_a which remains almost constant down to 9.5 K and, consequently, the corresponding opposite variation must be ascribed to I_c. The rotation axis in this temperature range would be near the a direction. The difficulty in obtaining OA spectra along the three orthorhombic directions in a given crystal plate during the same cooling cycle prevents us from confirming this statement. It must be noted, however, that the $I(T)$ curves in figure 4 correspond to the highest variations found among all the investigated crystal plates. Different variations observed in other b and c plates are weaker and smoother than that in figure 4. This behaviour is probably due to the distinct domain structure displayed by each crystal in the monoclinic phase. The weakest intensity variation should be expected for crystals having the two types of monoclinic domain equally distributed. The results in figure 4 can be well explained on the assumption that one of the domains is preponderant. In such case, the *relative band C intensity* $I_r = I_a/(I_a + I_b)$ gives directly $\cos^2\phi$, where $\phi = 40° + \Delta\phi$ is the angle that the projection of the distortion e_3 axis makes with the a direction. The inset of figure 4 shows the temperature dependence of the rotation angle $\Delta\phi$ derived from the measured intensities. Analogously with the findings for $CdBr_4^{2-}$ in the pure TMA_2CdBr_4 crystal [11], $CuBr_4^{2-}$ also experiences rotational motions with increasing temperature. The rotation angle is almost zero in the orthorhombic phase and progressively decreases just below the PT temperature $T_{c1} = 272$ K, reaching a minimum $\Delta\phi = -14°$ at 230 K. Below this temperature, the sense of rotation changes and $\Delta\phi$ rapidly increases to −3° at 150 K, where it remains almost constant. Note that no structural information can be obtained below 150 K since the rotation axis could itself rotate. According to the conclusions of [11], this change in $\Delta\phi$ at around 230 K does not seem to be associated with a new PT, but the shape of the variation resembles that followed by the monoclinic β parameter in the 70–300 K range.

An interesting aspect connected with these variations is the abrupt changes observed at 20 K (heating cycle) and at 10 K (cooling cycle) (figure 5). The inset shows the CT spectra at 15 and 25 K but obtained for a *b* plate. Note that the sign and magnitude of the variation of the *a* intensity are sample dependent and can change in the same sample for different heating–cooling runs. In particular, the spectra of the *b* plate clearly indicate that an abrupt rotation around the c axis takes place at $T = 20$ K. This dynamic, however, is not observed for the *c* plate where the intensities in both *a* and *b* polarizations sharply decrease above 20 K. Although this behaviour cannot be explained in terms of rotations around the *c* axis, the OA spectra obtained at around 20 K for several plates indicate that these variations correspond to rotations of the $CuBr_4^{2-}$ complex. Structural investigations to clarify the dynamics of the inorganic $CdBr_4^{2-}$ at low temperatures would be useful. In any case, the fact that we detect intensity jumps at the same temperature with the same thermal hysteresis permits us to conclude that such variations are induced by a new structural PT in TMA_2CdBr_4. In no case can these changes be ascribed to local effects since small abrupt changes in the crystal transmittance out of the CT absorption region (800 nm) are also observed at these temperatures. The existence of a new PT in the present system is also supported by the universal p–T phase diagram of the TMA_2MBr_4 (M = Zn, Co, Mn or Cd) crystal family, where a monoclinic-to-orthorhombic ($P2_1/c \rightarrow P2_12_12_1$) PT should exist below the high $Pmcn \rightarrow P2_1/c$ PT temperature at atmospheric pressure. Previous attempts to detect this PT in different bromides were unsuccessful probably because the unexpected low transition temperature was not explored [37]. Evidence of a low-temperature PT was given by Gesi [38] for TMA_2CuCl_4 through dielectric measurements. Nevertheless, the anomaly detected at 10 K was explained in terms of a possible antiferromagnetic PT but further work to clarify the nature of such an anomaly is required.

The observation of a new PT in TMA_2CdBr_4 at $T_{c2} = 20$ K through the CT spectra indicates the good sensitivity of optical spectroscopy for detecting PTs. In the present case, the band polarization proves to be useful for detecting PTs involving reorientations rather than geometrical distortions of the inorganic tetrahedra.

Acknowledgments

This work has been supported by Caja Cantabria and the CICYT (project PB92-0505).

References

[1] Bird B D and Day P 1968 *J. Chem. Phys.* **49** 392
[2] Rivoal J C and Briat B 1974 *Mol. Phys.* **27** 1081
[3] Stein P, Jensen P W and Spiro T G 1981 *Chem. Phys. Lett.* **80** 451
[4] Marco de Lucas M C and Rodríguez F 1993 *J. Phys.: Condens. Matter* **5** 2625
[5] Aramburu J A, Moreno M and Bencini A 1987 *Chem. Phys Lett.* **140** 462
[6] Marco de Lucas M C, Rodríguez F and Aramburu J A 1991 *J. Phys.: Condens. Matter* **3** 8945
[7] Valiente R, Marco de Lucas M C and Rodríguez F 1994 *J. Phys.: Condens. Matter* **6** 4527
[8] Sato S, Ikeda R and Nakamura D 1986 *Bull. Chem. Soc. Japan* **59** 1981
[9] Vanek P, Havrankova M and Smutny F 1991 *Solid State Commun.* **77** 169
[10] Gesi K 1992 *Phase Transitions* A **38** 1
[11] Asahi T, Hasabe K and Gesi K 1992 *J. Phys. Soc. Japan* **61** 1590
[12] Perret R, Godefroy G and Arend H 1987 *Ferroelectrics* **73**
[13] Shimizu H 1980 *J. Phys. Soc. Japan* **49** 223
[14] Gesi K 1982 *J. Phys. Soc. Japan* **51** 2532
[15] Yamada Y and Hayama N 1983 *J. Phys. Soc. Japan* **52** 3466

[16] Marco de Lucas M C and Rodríguez F 1992 *Ferroelectrics* **125** 159
[17] Breñosa A G, Moreno M, Rodríguez F and Couzi M 1991 *Phys. Rev.* B **44** 9859
[18] Breñosa A G, Moreno M and Rodríguez F 1987 *Solid State Commun.* **63** 543
[19] Rodríguez F, Breñosa A G, Aramburu J A, Moreno M and Calleja J M 1987 *J. Phys. C: Solid State Phys.* **20** L641
[20] Breñosa A G, Rodríguez F and Moreno M 1988 *J. Phys. C: Solid State Phys.* **21** L623
[21] Breñosa A G, Rodríguez F and Moreno M 1990 *Ferroelectrics* **106** 187
[22] Breñosa A G, Rodríguez F and Moreno M 1993 *Solid State Commun.* **85** 135
[23] Valiente R, Marco de Lucas M C, Espeso J I and Rodríguez F 1993 *Solid State Commun.* **86** 663
[24] Smith D W 1976 *Coord. Chem. Rev.* **21** 93
[25] Battaglia L P, Bonamartini Corradi A, Marcotrigiano G, Menabue L and Pellacini G C 1979 *Inorg. Chem.* **18** 148
[26] Bond M R, Johnson T J and Willet R D 1988 *Can. J. Chem.* **66** 963
[27] Harlow R L, Wells W J, Watt G W and Simonsen S H 1974 *Inorg. Chem.* **13** 2106
[28] Halvorson K E, Patterson C and Willet R D 1990 *Acta. Crystallogr.* B **46** 508
[29] Morosin B and Lingafelter E C 1960 *Acta. Crystallogr.* **13** 807
[30] Hasebe K, Mashiyama H and Tanisaki S 1985 *Japan. J. Appl. Phys.* **24** 758
[31] Asahi T, Hasebe K and Gesi K 1988 *J. Phys. Soc. Japan* **57** 4219
[32] Madariaga G, Zúñiga F J, Paciorek W A and Bocanegra E H 1990 *Acta Crystallogr.* B **46** 620
[33] Gesi K 1983 *J. Phys. Soc. Japan* **52** 2931
[34] Torgashev V I, Yuzyuk Y I, Burmistrova L A, Smutny F and Vanek P 1994 *J. Phys.: Condens. Matter* **6** 4527
[35] Lamba O P and Sinha S K 1986 *Solid State Commun.* **57** 365
[36] Hitchman M A 1994 *Comment. Inorg. Chem.* **15** 197
[37] Gesi K 1982 *J. Phys. Soc. Japan* **51** 203
[38] Gesi K 1989 *Ferroelectrics* **96** 195